Systematic study of α-decay energies and half-lives of superheavy nuclei

Y. Z. Wang (王艳召),[1,2,3,*] S. J. Wang (王少敬),[1] Z. Y. Hou (侯召宇),[1,2,†] and J. Z. Gu (顾建中)[3,‡]
[1]*Department of Mathematics and Physics, Shijiazhuang Tiedao University, Shijiazhuang 050043, China*
[2]*Institute of Applied Physics, Shijiazhuang Tiedao University, Shijiazhuang 050043, China*
[3]*China Institute of Atomic Energy, P.O. Box 275 (10), Beijing 102413, China*
(Received 19 October 2015; published 3 December 2015)

Systematic calculations on the α-decay energies (Q_α) and α-decay half-lives of the superheavy nuclei (SHN) with $Z \geqslant 100$ are performed by using 20 models and 18 empirical formulas, respectively. According to the comparisons between the calculated results and experimental data, it is shown that the WS4 mass model is the most accurate one to reproduce the experimental Q_α values of the SHN. Meanwhile it is found that the SemFIS2 formula is the best one to predict the α-decay half-lives of the SHN because the parameters in this formula are from the experimental α emitter data of transuranium nuclei including SHN ($Z = 92$–118). In addition, the UNIV2 formula with fewest parameters and the VSS, SP and NRDX formulas with fewer parameters work well in prediction on the SHN α-decay half-lives. Finally, the α-decay half-lives of $Z = 110$–120 isotopes are predicted within the above mentioned five formulas by inputting the WS4 Q_α values. By analyzing the Q_α values and the α-decay half-lives of this region, it is found that for $Z = 110$–114 isotopes $N = 162$ and $N = 184$ are the submagic number and magic number, respectively. However, for the isotopes of $Z = 116$–120 the submagic number is $N = 178$.

DOI: 10.1103/PhysRevC.92.064301 PACS number(s): 23.60.+e, 21.10.Dr, 21.10.Tg, 27.90.+b

I. INTRODUCTION

α radioactivity was first observed by Rutherford and Geiger at the beginning of the last century. Twenty years later, it was described successfully by Gamow [1] and by Condon and Gurney [2] as a quantum tunneling effect. Since then, on the basis of Gamow's picture many phenomenological and microscopic models have been developed to calculate α-decay half-lives [3–13]. In addition to these models, several empirical formulas, which are dependent on the α-decay energies (Q_α), charge number Z, and/or mass number A of nuclei, have been proposed to compute α-decay half-lives [8,14–23]. Using these formulas, α-decay half-lives can be estimated easily and rapidly. Especially they are usually used to predict half-lives where the experimental values are unavailable, to serve experimental design [24]. In predictions with the empirical formulas it is well known that Q_α values play a crucial role in determining half-lives. Half-lives are extremely sensitive to the Q_α values. An uncertainty of 1 MeV in Q_α leads to an uncertainty of α-decay half-life ranging from 10^3 to 10^5 times for heavy nuclei. So it is very important and necessary to obtain the accurate Q_α values. In recent years, great efforts have been made to predict accurate Q_α values. Usually Q_α values are obtained by two types of methods. On the one hand, one derives Q_α formulas by fitting the experimental Q_α data based on the liquid drop model [25,26]. On the other hand, many different nuclear mass models were developed by phenomenological and microscopic methods [27–45]. By using the relationship between the $Q_\alpha(Z,N)$ value and nuclear mass excess $M(Z,N)$,

$$Q_\alpha(Z,N) = M(Z,N) - M(Z-2,N-2) - M(2,2), \quad (1)$$

Q_α values can be derived. Concerning predictions of α-decay half-lives, many studies have been done within various empirical formulas by inputting different types of Q_α values [8,26,46–56]. According to these studies, it is found that (i) for a given nucleus different empirical formulas lead to different predictions although the Q_α value is the same; (ii) when one extracts the Q_α values, large differences between different methods are found. This drives us to suspect the reliability of these predictions. We think that if one wants to give reliable predictions of α-decay half-lives, the selection of the empirical formulas and Q_α values becomes extremely important. So it is necessary to test the accuracies of Q_α values from different methods and the predictive abilities of the empirical formulas. This constitutes the motivation of this article.

Nowadays, the study of superheavy nuclei (SHN) is an interesting and popular subject in nuclear physics [57–65]. Studies suggest that α-decay is one of the most important decay modes for SHN and has become a powerful tool to identify new elements via the observation of α-decay chains [57–65]. In recent decades many superheavy elements or isotopes have been synthesized by hot, warm, and cold fusion reactions. Meanwhile, a lot of experimental data on the Q_α values and α-decay half-lives of SHN have been measured [57–65], which can be therefore used to examine the Q_α accuracies and the empirical formulas' predictive abilities from different methods. In addition, we know that the mass of an atomic nucleus is one of the basic quantities, which plays important roles not only in various aspects of nuclear physics but also in astrophysics [66]. Very recently, the predictive power of many nuclear mass models has been studied by comparing with the existing experimental data of nuclear masses [67]. However, for most SHN their masses are not yet measured. Thus the

*yanzhaowang09@126.com
†houzhaoyu@stdu.edu.cn
‡gujianzhong2000@aliyun.com

experimental Q_α values of SHN provide us a testing ground for various nuclear mass models. In this article we calculate the Q_α values and α-decay half-lives of SHN with $Z \geqslant 100$ by using various approaches. By comparison between the calculated values and experimental data, we try to find the most accurate methods to calculate Q_α values and the most reliable empirical formulas to compute α-decay half-lives. This article is organized in the following way. In Sec. II the theoretical framework is introduced. The numerical results and corresponding discussions are given in Sec. III. In the last section, some conclusions are drawn.

II. THEORETICAL FRAMEWORK

A. Methods of extracting Q_α values

To calculate the Q_α values of heavy nuclei and SHN with a high precision, two simple fitting formulas have been proposed based on the local liquid drop model [25,26], which are expressed as

$$Q_\alpha = aZA^{-4/3}(3A-Z) + b\left(\frac{N-Z}{A}\right)^2 + c\left[\frac{|N-152|}{N} - \frac{|N-154|}{N-2}\right] + d\left[\frac{|Z-110|}{Z} - \frac{|Z-112|}{Z-2}\right] + e, \quad (2)$$

$$Q_\alpha = a_1 + \frac{a_2}{A^{1/3}} + a_3\frac{Z}{A^{1/3}}\left(1-\frac{Z}{3A}\right) + a_4\left(\frac{N-Z}{A}\right)^2 + a_5\left[1-\left(\frac{N-154}{a_6}\right)^2\right]\exp\left[-\frac{1}{2}\left(\frac{N-154}{a_6}\right)^2\right] + a_7\left[1-\left(\frac{N-164}{a_8}\right)^2\right]\exp\left[-\frac{1}{2}\left(\frac{N-164}{a_8}\right)^2\right]. \quad (3)$$

In Eqs. (2) and (3), the parameters (a,b,c,d,e) and $(a_1,\ldots,a_8)$ are fitted by the experimental Q_α values with ($Z \geqslant 90$, $N \geqslant 140$) and ($Z \geqslant 92$, $N \geqslant 140$), respectively [25,26]. The Q_α values in these mass regions are well reproduced by the two formulas.

In recent years many nuclear mass models, such as macroscopic-microscopic models [27–33], microscopic models based on the mean-field concept [34–40], and other kinds of models [41–45], have been developed with rms deviations from several hundred keV to a few MeV with respect to all known nuclear masses. In nuclear mass models that include Eq. (1), the Q_α values can be obtained.

B. Empirical formulas for determining α-decay half-lives

Analytic formulas, such as the Royer formula [8], Viola-Seaborg-Sobiczewski (VSS) formula [14,15], Sobiczewski-Parkhomenko (SP) formula [16,17], Ni-Ren-Dong-Xu (NRDX) formula [18], Horoi formula [19], and Santhosh formula [20] are usually used to evaluate and predict the α-decay half-lives. These formulas are written as follows:

$$\log_{10} T_{1/2}(\text{Royer}) = a + bA^{1/6}Z^{1/2} + cZQ_\alpha^{-1/2}, \quad (4)$$

$$\log_{10} T_{1/2}(\text{VSS}) = (aZ+b)Q_\alpha^{-1/2} + cZ + d + h, \quad (5)$$

$$\log_{10} T_{1/2}(\text{SP}) = aZ(Q_\alpha - \overline{E_i})^{-1/2} + bZ + c, \quad (6)$$

$$\log_{10} T_{1/2}(\text{NRDX}) = a\sqrt{\mu}Z_\alpha Z_d Q_\alpha^{-1/2} + b\sqrt{\mu}(Z_\alpha Z_d)^{1/2} + c, \quad (7)$$

$$\log_{10} T_{1/2}(\text{Horoi}) = (a_1\mu^x + b_1)\left[(Z_\alpha Z_d)^y Q_\alpha^{-1/2} - 7\right] + (a_2\mu^x + b_2), \quad (8)$$

$$\log_{10} T_{1/2}(\text{Santhosh}) = aQ_\alpha^{-1/2} + b\eta_A + c, \quad (9)$$

where $T_{1/2}$ is the calculated α partial half-life measured in seconds and Q_α is measured in MeV. Z, Z_d, and Z_α are the proton numbers of the parent nucleus, residual daughter nucleus, and α particle, respectively. $\mu = A_\alpha A_d/(A_\alpha + A_d)$ is the reduced mass. A_α and A_d denote the mass numbers of the α particle and residual daughter nucleus. In the VSS formula the parameter h represents the hindrances associated with the unpaired nucleons. The parameter $\overline{E_i}$ in Eq. (6) represents the average excitation energy of a state of the daughter nucleus to which the α decay goes, which is also in MeV. In Eq. (9) $\eta_A = (A_d - A_\alpha)/A$ denotes the mass asymmetry. These parameters (a, b, c, d, h, $\overline{E_i}$, a_1, a_2, b_1, b_2, x, y) are determined by fitting to experimental half-lives of α decay. These parameters can be found in relevant references [8,14–20].

Later Schubert *et al.* rederived a set of new coefficients for the Royer formula, the VSS formula, and the SP formula by using the reliable data of the α-standard nuclei [68]. The three formulas with the new sets of coefficients were renamed the Rm, VSm, and SPm formulas. Note that there are two versions for the VSm formula and the SPm formula: they are (VSm1, VSm2) and (SPm1, SPm2), respectively. For the case of VSm2, the h factor was merged into the parameter d [68]. These new values of the coefficients for even-even (e–e), even-odd (e–o), odd-even (o–e), and odd-odd (o–o) nuclei are listed in the Table II of Ref. [68].

In addition to the simple analytic formulas mentioned above, some semi-empirical relationships including microscopic effects, such as the universal (UNIV) curve [69], and a semi-empirical formula based on fission theory (SemFIS) [69], were proposed by Poenaru *et al*. The UNIV formula for e-e nuclei is written as

$$\log_{10} T_{1/2}(s) = -\log_{10} P + c_{ee}. \quad (10)$$

In Eq. (10) the penetrability P of an external part of the barrier, having separation distance at the touching configuration $R_a = R_t = R_d + R_\alpha$ as the first turning point and the second one defined by $e^2 Z_d Z_\alpha / R_b = Q_\alpha$, may be found analytically as

$$-\log_{10} P = 0.22873(\mu Z_d Z_\alpha R_b)^{1/2} \times [\arccos\sqrt{r} - \sqrt{r(1-r)}], \quad (11)$$

where $r = R_t/R_b$, $R_t = 1.2249(A_d^{1/3} + A_\alpha^{1/3})$, and $R_b = 1.43998 Z_d Z_\alpha / Q_\alpha$.

The additive constant of Eq. (10) $c_{ee} = \log_{10}S_\alpha - \log_{10}\nu + \log_{10}(\ln 2)$. Here S_α and ν represent the preformation probability of the α particle at the nuclear surface and the frequency of assaults on the barrier per second, respectively. $c_{ee} = -20.325$ by the following two approximations: $S_\alpha = 0.0180302$ and $\nu = 10^{22.01}$ s^{-1}. For e-o, o-e, and o-o nuclei c_{ee} is replaced by $c_{eo} = c_{ee} + h_{eo}$, $c_{oe} = c_{ee} + h_{oe}$, and $c_{oo} = c_{ee} + h_{oo}$, respectively, where h_{eo}, h_{oe}, and h_{oo} are the mean values of the hindrance factors in these groups of nuclides. These values can be found from Ref. [69].

For the SemFIS formula is expressed as

$$\log_{10} T_{1/2}(s) = 0.43429K_S\chi(x,y) - 20.446 + H^f, \quad (12)$$

where

$$K_S = 2.52956Z_d[A_d/(AQ_\alpha)]^{1/2} \times[\arccos\sqrt{r} - \sqrt{r(1-r)}] \quad (13)$$

and $r = 0.423Q_\alpha(1.5874 + A_d^{1/3})/Z_d$.

The numerical coefficient $\chi(x,y)$, close to unity, is a second-order polynomial:

$$\chi(x,y) = B_1 + x(B_2 + xB_4) + y(B_3 + yB_6) + xyB_5. \quad (14)$$

The $B_i (i = 1,2,\ldots,6)$ parameters are obtained by fitting the data of e-e α emitters. The reduced variables x and y are defined as

$$\begin{aligned} x &\equiv (N - N_i)/(N_{i+1} - N_i), \quad N_i < N \leqslant N_{i+1}, \\ y &\equiv (Z - Z_i)/(Z_{i+1} - Z_i), \quad Z_i < Z \leqslant Z_{i+1}, \end{aligned} \quad (15)$$

with $N_i = \ldots,51,83,127,185,229,\ldots$, $Z_i = \ldots,29,51,83,127,\ldots$; hence for the region of SHN $x = (N-127)/(185-127)$, $y = (Z-83)/(127-83)$. In formula (12) H^f is a hindrance factor which takes different values for e-e, e-o, o-e, and o-o nuclei [69].

In Ref. [69] the parameters of UNIV and SemFIS formulas are obtained by fitting the experimental α emitter data of two regions of the nuclear chart. One region is 493 α emitters with $Z = 52$–118; another one is 142 transuranium nuclei including superheavies ($Z = 92$–118). In this article the formulas from $Z = 52$–118 nuclei are named the UNIV1 and SemFIS1 formulas. The formulas from $Z = 92$–118 nuclei are named the UNIV2 and SemFIS2 formulas.

The favored α decay, where the orbital angular momentum taken by the α particle is $l = 0$, can be analyzed by the empirical formulas mentioned above. However, for the unfavored case, the l dependence should be taken into account. New expressions including the l-dependent terms have been recently proposed [22,23,70–73] and the dependence on the excitation energy has been studied [53–55,70,73–75]. The formulas for evaluating the unfavored ground state to ground state transitions proposed by Denisov [22] and Royer [23] are written as follows:

$$\log_{10} T_{1/2}(\text{Denisov}) = a + b(A-4)^{1/6}Z^{1/2} + cZQ_\alpha^{-1/2} + dl(l+1)^{1/2}Q_\alpha^{-1}A^{1/6} + e[(-1)^l - 1], \quad (16)$$

$$\log_{10} T_{1/2}(\text{Royer10}) = a + bA^{1/6}Z^{1/2} + cZQ_\alpha^{-1/2} + dANZl(l+1)^{1/4}Q_\alpha^{-1} + eA[1-(-1)^l]. \quad (17)$$

The parameters (a,b,c,d,e) in Eqs. (16) and (17) were obtained by fitting the experimental data for half-lives in 344 α emitters [22,23]. It is known that the ground-state spins and parities of e-e nuclei are 0^+. For the e-o, o-e, and o-o SHN the spins and parities of parent and daughter nuclei are unknown. Therefore, usually the l contribution is not considered in the calculations. With $l = 0$ the form of Eq. (16) is changed as

$$\log_{10} T_{1/2}(\text{Denisov}) = a + b(A-4)^{1/6}Z^{1/2} + cZQ_\alpha^{-1/2}. \quad (18)$$

Equation (17) is the same as Eq. (4) except for the fitting parameters. To distinguish the difference between the two formulas, Eq. (17) is called the Royer10 formula in this article. In addition, the coefficients in the Denisov formula were recalculated by Royer [23]. Thus the Denisov formula with the coefficients of Refs. [22] and [23] are renamed the Densiov1 formula and the Densiov2 formula, respectively.

III. RESULTS AND DISCUSSIONS

We have extracted the Q_α values of the 121 SHN with $Z \geqslant 100$ using Eqs. (2) and (3) and the nuclear masses. These nuclear masses are from different models, which include the finite-range droplet model (FRDM) [27]; the finite-range liquid-drop model (FRLDM) [27]; the newest Weizsäcker-Skyrme (WS) model [31]; the simple nuclear mass formula (SNMF) proposed recently by Bhagwat [32]; the extended Bethe-Weizsäcker (EBW) formula [33]; the Hartree-Fock-Bogoliubov mean-field model with the BSk28 and BSk29 Skyrme interactions (HFB28, HFB29) [34] and with the D1S Gogny force (GHFB) [35]; the extended Thomas-Fermi plus Strutinsky integral (ETFSI) method [37]; the extended Thomas-Fermi approach based on the Skyrme energy density functional (ETFSEDF) [38]; the Duflo-Zuker (DZ) model [41,42]; the Kourra-Tachibaba-Uno-Yamada (KTUY) formula [43]; and the infinite nuclear matter model (INMM) [44]. Note that the newest WS model was called the WS4 model in Ref. [31]. In calculations of the Q_α values with the DZ model, the masses of DZ10 [41], optimized DZ10 [41], DZ19 [42], DZ28 [41], DZ31 [42], and DZ33 [42] are used. Here 10, 19, 28, 31, and 33 denote the numbers of the fitting parameters. To show the global deviation between the experimental and calculated Q_α values, the average deviation and standard deviation are calculated by the expressions

$$\overline{\sigma} = \frac{1}{121}\sum_{i=1}^{121}\left|Q_\alpha^i(\text{expt.}) - Q_\alpha^i(\text{cal.})\right|, \quad (19)$$

$$\sqrt{\sigma^2} = \sqrt{\sum_{i=1}^{121}\frac{\left[Q_\alpha^i(\text{expt.}) - Q_\alpha^i(\text{cal.})\right]^2}{121}}. \quad (20)$$

The calculated values of the average deviation $\overline{\sigma}$ and standard deviation $\sqrt{\sigma^2}$ for the 121 SHN Q_α values from 20 different models are listed in Table I. From Table I, one can see

TABLE I. The $\overline{\sigma}$ and $\sqrt{\sigma^2}$ values of Q_α obtained from 20 different models. These experimental Q_α values are taken from [57–65,76–89].

Model	$\overline{\sigma}$ (MeV)	$\sqrt{\sigma^2}$ (MeV)
Formula 2 [25]	0.224	0.317
Formula 3 [26]	0.209	0.273
FRDM [27]	0.303	0.420
FRLDM [27]	0.296	0.388
WS4 [31]	0.177	0.219
SNMF [32]	0.395	0.530
EBW [33]	0.912	1.105
HFB28 [34]	0.393	0.538
HFB29 [34]	0.370	0.505
GHFB [35]	0.457	0.617
ETFSI [37]	0.443	0.519
ETFSEDF [38]	0.731	0.813
DZ10 [41]	0.595	0.737
Optimized DZ10 [42]	0.587	0.732
DZ19 [42]	0.535	0.651
DZ28 [41]	0.494	0.658
DZ31 [41]	0.743	0.902
DZ33 [42]	0.728	0.878
KTUY [43]	0.286	0.352
INMM [44]	0.534	0.758

that different models generate different $\overline{\sigma}$ and $\sqrt{\sigma^2}$ values. This indicates that the extracted Q_α values are dependent strongly on the models. In addition, it is seen that the WS4 model has the smallest $\overline{\sigma}$ and $\sqrt{\sigma^2}$ values, which indicates that it is the most accurate model to reproduce the experimental Q_α values of the SHN. To see the deviation between the experimental and calculated Q_α values more clearly, the values of $Q_\alpha^i(\text{expt.}) - Q_\alpha^i(\text{cal.})$ as functions of the neutron number N for different models are plotted in Fig. 1. From Fig. 1 it is seen that the deviation from the WS4 model is the smallest by comparing the $Q_\alpha^i(\text{expt.}) - Q_\alpha^i(\text{cal.})$ distributions for different models, which is consistent with the calculated results in Table I. Although the WS model is a semi-empirical one, it is proposed by combining the advantages of the macroscopic-microscopic model and the Skyrme energy density functional. In the process of determining the model parameters, many important physical features, such as the mirror nuclei effect due to isospin symmetry, the Wigner-like effect from the symmetry between valence protons and valence neutrons, the corrections for pairing effects, and the triaxial deformation, are considered so that the experimental nuclear masses can be reproduced precisely [30]. Especially for the recent WS4 model, by taking into account the surface diffuseness correction for unstable nuclei, its accuracy is further improved [31]. The rms deviation with respect to the 2353 known masses falls to 298 keV, crossing the 0.3 MeV accuracy threshold for the first time within the mean-field approximation. For formulas (2) and (3), it is seen in Table I that they produce smaller $\overline{\sigma}$ and $\sqrt{\sigma^2}$, which suggests that the two formulas can be used to make a prediction for the Q_α values of the SHN with good accuracy, although they are not the most accurate models. By comparing the values of $\overline{\sigma}$ and $\sqrt{\sigma^2}$ given by the two formulas, it is found that formula 3 works better than formula 2 due to introducing more fitting parameters. Regarding the accuracy of the description of nuclear masses, it is well known that the FRDM is better than the FRLDM [27]. However, the evaluations in Table I suggest that the accuracy of the FRDLM is better than that of the FRDM in the Q_α predictions of the SHN. For the SNMF model, Ref. [32] claimed that the model yields an rms deviation of 266 keV from 2353 known nuclear masses. As far as we know it could be the most accurate model to predict nuclear masses. However, our calculated values of $\overline{\sigma}$ and $\sqrt{\sigma^2}$ in Table I and the $Q_\alpha^i(\text{expt.}) - Q_\alpha^i(\text{cal.})$ distributions in Fig. 1 show that the SNMF is not the best model to estimate the Q_α values of the SHN. Because of the complexity of the structures of the SHN, it is difficult to reliably describe the fluctuating part of the ground-state energy by the simple parametrization approach. These facts tell us that the nuclear mass models that have strong predictive power may not give the Q_α values of the SHN precisely. As can be seen from Table I and Fig. 1, for the microscopic models the best accuracy for Q_α values of the SHN is obtained by the HFB29 model. By comparing to the accuracy of the HFB28 model it is found that the predictive power of HFB29 is further improved. For other kinds of models, which are referred to as the DZ, KTUY, and INMM models in this article, from Table I and Fig. 1 we know easily that the smallest deviation is from the KTUY model. In addition, we can see that the optimized DZ10 model improves the accuracy compared to the DZ10 model by fitting the latest experimental data from Ref. [76].

We note that the search for the magic numbers of the SHN has been an interesting subject [25,26,76]. With the Q_α values the magic numbers can be deduced. Because the most accurate Q_α values are from the WS4 model, it is helpful to predict the magic numbers by the WS4 Q_α values. The Q_α values of $Z = 110$–120 isotopes obtained from the WS4 model versus N are shown in Fig. 2. From Fig. 2 one can see that, for the $Z = 110$–114 isotopes, $N = 162$ and 184 are the submagic number and magic number, respectively. However, for the isotopes of $Z = 116$ and 118 the submagic number at $N = 162$ is replaced by $N = 178$. Meanwhile, the closed shell effect of at $N = 184$ is weakened a lot. For the $Z = 120$ isotopes, the Q_α minimums are located at $N = 178$ and 184, respectively. Furthermore, the closed shell effect of $N = 184$ is stronger than that of $N = 178$.

Next we will discuss the α-decay half-lives of the SHN by various analytic formulas. We have performed the calculations on the α-decay half-lives of the 99 SHN with $Z \geqslant 100$ by the Royer, VSS, SP, NRDX, Horoi, Santhosh, UNIV1, UNIV2, SemFIS1, SemFIS2, Rm, VSm1, VSm2, SPm1, SPm2, Royer10, Denisov1, and Denisov2 formulas by inputting the experimental Q_α values. Note that in the calculations using the Denisov 1 formula, the Set I parameters in Ref. [22] are used. Usually the ratio between the experimental α-decay half-life and calculated one is applied to analyze the accuracy degree of models, whose decimal logarithm form is written as

$$\log_{10} R = \log_{10} \frac{T_{1/2}^{\text{expt.}}}{T_{1/2}^{\text{cal.}}}. \tag{21}$$

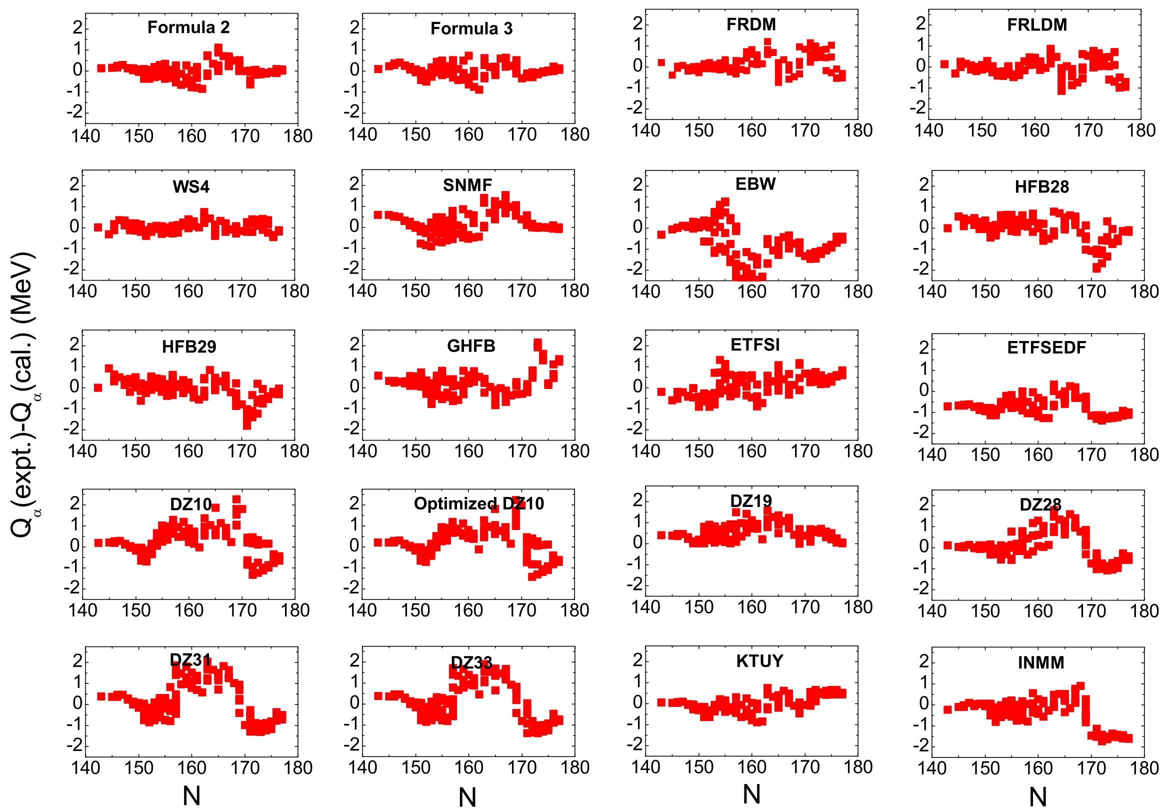

FIG. 1. (Color online) The deviations between experimental and calculated Q_α values as functions of the neutron number N for 20 different models.

Regarding Eq. (21), usually one thinks that if the $\log_{10} R$ value is within a factor of 1.0, the calculated half-lives will be in agreement with the experimental data. Recently Ref. [17] introduced the factor of average discrepancy $\overline{\delta}$ to describe the predictive ability of the α-decay half-life formulas. The average discrepancy $\overline{\delta}$ is defined as

$$\overline{\delta} = \frac{1}{N} \sum_{i=1}^{N} \left| \log_{10} \frac{T_{1/2}^{\text{cal.}}}{T_{1/2}^{\text{expt.}}} \right|. \tag{22}$$

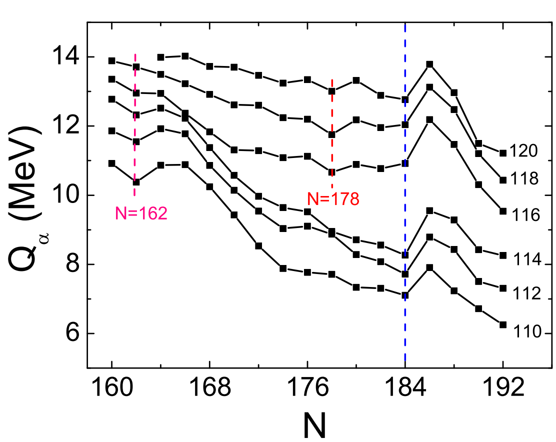

FIG. 2. (Color online) The Q_α values of $Z = 110$–120 isotopes as a function of N for WS4 model.

By using Eq. (22) the $\overline{\delta}$ form is changed as

$$\overline{\delta} = \frac{1}{N} \sum_{i=1}^{N} |\log_{10} R|. \tag{23}$$

Equation (23) tells us that the smaller $\overline{\delta}$ is, the better the formula is. With Eq. (23) the $\overline{\delta}$ values of the 18 different analytic formulas can be obtained, which are listed in Table II. For ease of discussion, the number of parameters for each formula is also listed in Table II. In addition, to see the deviation between the experimental half-lives and calculated ones more clearly, the $\log_{10} R$ values as functions of N for the 18 different analytic formulas are shown in Fig. 3. From Table II and Fig. 3, one can see that the SemFIS2 formula has the smallest $\overline{\delta}$ value and the $\log_{10} R$ values constrained within a factor of 1.0 are more than other kinds of formulas. This indicates that the SemFIS2 formula is the best one to predict the α-decay half-lives of the SHN. This is because the fitting parameters in this formula are from the experimental data of α decay of transuranium nuclei including SHN ($Z = 92$–118). For this reason the accuracy degrees of UNIV2 and SemFIS2 formulas are improved a lot by comparisons to the UNIV1 and SemFIS1 formulas. Besides this, the experimental half-lives are well reproduced by the UNIV2 formula although the fewest parameters are contained. In addition to the UNIV2 and SemFIS2 formulas, other kinds of formulas are widely used to calculate the α-decay half-lives in the whole nuclear chart. For other kinds of formulas as can be seen from Table II we find that the

TABLE II. The parameter numbers and the $\bar{\delta}$ values of α-decay half-lives from 18 different analytic formulas. These experimental α-decay half-lives are taken from [57–65,76–89].

Formula	Number of parameters	$\bar{\delta}$
Royer [8]	12	0.673
VSS [14,15]	7	0.534
SP [16,17]	6	0.529
NRDX [18]	7	0.518
Horoi [19]	6	0.812
Santhosh [20]	3	0.764
UNIV1 [69]	4	0.722
UNIV2 [69]	4	0.546
SemFI1 [69]	12	0.574
SemFI2 [69]	12	0.505
Rm [68]	12	0.762
VSm1 [68]	7	0.575
VSm2 [68]	16	1.797
SPm1 [68]	6	0.797
SPm2 [68]	15	2.474
Royer10 [23]	12	0.568
Denisov1 [22]	12	0.578
Denisov2 [23]	12	0.537

VSS, SP, NRDX, SemFIS1, VSm1, Royer10, Denisov1, and Densiov2 formulas give smaller $\bar{\delta}$ values, which shows that to some extent these formulas can be used to predict the α-decay half-lives of the SHN. Among these formulas, the VSS, SP, and NRDX formulas including the fewest parameters have the best predicted abilities. In Ref. [68] the Rm, VSm, and SPm formulas were tested against the experimental half-lives of 235 nuclei. It was found that these new formulas work well. However, when tested against the superheavy elements and the medium-mass α emitters, the predicted abilities of the Rm and m2 formulas are worse than those of the old formulas, which is consistent to the results of Table II. As can be seen from Table II and Fig. 3, we know that not only the accuracy degree of the m2 formulas is less than the one of the m1 formulas but also the m2 formulas are the worst ones to predict the α-decay half-lives of the SHN, although more parameters are included. In addition, the Royer, Royer10, Denisov1, and Denisov2 formulas are all 12-parameter ones. According to the comparisons between them, we know that the predictive powers of the Royer10 and Denisov2 formulas are better than those of the Royer and Denisov1 formulas, respectively.

By the analysis and discussions on the Q_α values and α-decay half-lives of the SHN from various models, we find that the most accurate model to reproduce the experimental Q_α values and the most reliable formulas to estimate the α-decay half-lives are the WS4 model and the SemFIS2 formula, respectively. In addition, the UNIV2 formula with the fewest parameters and the VSS, SP, and NRDX formulas with fewer parameters have high predictive abilities. With the five formulas, by inputting the WS4 Q_α values, the α-decay half-lives with the $Z = 110$–120 isotopes are calculated, and

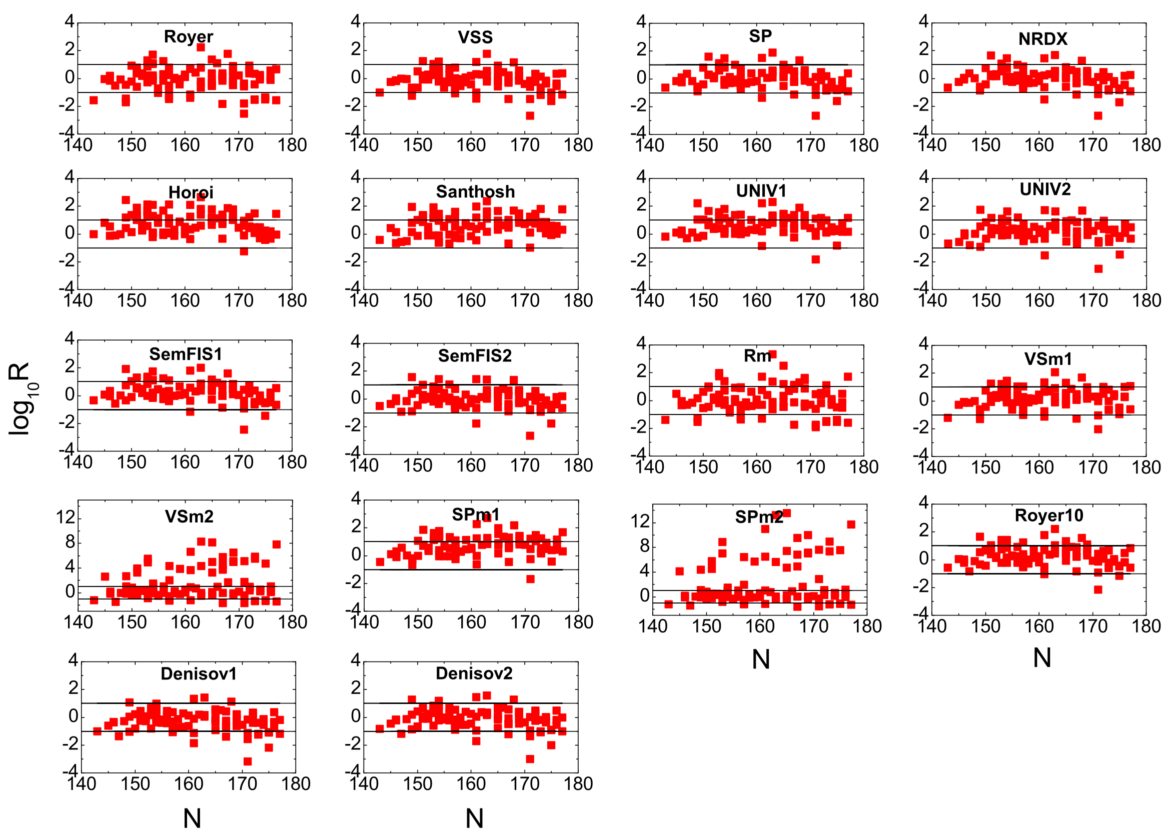

FIG. 3. (Color online) The values of $\log_{10}R$ as functions of N for 18 different analytic formulas.

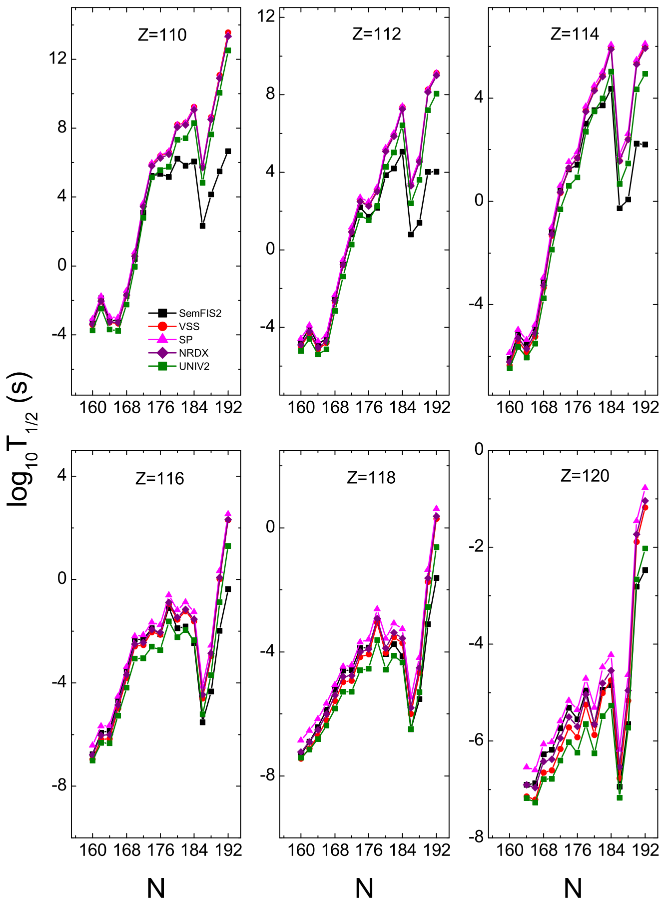

FIG. 4. (Color online) The predicted decimal logarithm of α-decay half-lives of the $Z = 110$–120 isotopes as functions of N for the SemFIS2, VSS, SP, NRDX, and UNIV2 formulas.

their decimal logarithm values as functions of N are plotted in Fig. 4. According to these predictions shown in Fig. 4, some information on the magic numbers of SHN can be observed, which is the same as the conclusion extracted from Fig. 2.

IV. CONCLUSIONS

In this article the Q_α values and α-decay half-lives of the SHN with $Z \geqslant 100$ have been calculated by using 20 models and 18 empirical formulas, respectively. By comparisons between the calculated results and experimental data, it is shown that (i) the WS4 mass model is the most accurate one to reproduce the experimental Q_α values of the SHN; (ii) although some nuclear mass models, such as FRDM and SNMF, have higher accuracy to reproduce the measured nuclear masses, they may not describe the Q_α values of the SHN precisely; (iii) because the parameters in the SemFIS2 formula are from the experimental α emitter data of transuranium nuclei including SHN ($Z = 92$–118), it is the best one to predict the α-decay half-lives of the SHN; (iv) the UNIV2 formula with fewest parameters and the VSS, SP, and NRDX formulas with fewer parameters work well in prediction of the SHN α-decay half-lives. Finally, the α-decay half-lives of $Z = 110$–120 are predicted within the SemFIS2, VSS, SP, NRDX, and UNIV2 formulas by inputting the Q_α values extracted from the WS4 mass model. By analyzing the WS4 Q_α values and the predicted α-decay half-lives of this region within the above mentioned five formulas, it is found that in the $Z = 110$–114 isotopes 162 and 184 are the neutron submagic number and neutron magic number, respectively. However, regarding the $Z = 116$–120 isotopes the possibility of the submagic number effect at $N = 178$ becomes evident, and should receive attention by researchers.

ACKNOWLEDGMENTS

We thank Prof. Ning Wang, Prof. S. G. Zhou, Prof. G. Royer, and Dr. J. M. Dong for helpful discussions, and Prof. Kirson for providing us the EBW mass table. This work was supported by the National Natural Science Foundation of China (Grants No. 11305109 and No. 11275271), the Funds for Creative Research Groups of China (No. 11321064), the Natural Science Foundation of Hebei Province of China (Grants No. A2012210043 and No. A2014210005), and the Research Foundation for College Outstanding Young Scholars of Hebei Province (Grant No. BJ2014052).

[1] G. Gamow, Z. Phys. **51**, 204 (1928).
[2] E. U. Condon and R. W. Gurney, Nature (London) **122**, 439 (1928).
[3] D. S. Delion and A. Sandulescu, J. Phys. G: Nucl. Part. Phys. **28**, 617 (2002).
[4] R. G. Lovas, R. J. Liotta, K. Varga, and D. S. Delion, Phys. Rep. **294**, 265 (1998).
[5] P. E. Hodgson and E. Běták, Phys. Rep. **374**, 1 (2003).
[6] B. Buck, A. C. Merchant, and S. M. Perez, At. Data Nucl. Data Tables **54**, 53 (1993).
[7] J. Wauters, P. Dendooven, M. Huyse, G. Reusen, P. Van Duppen, and P. Lievens (ISOLDE Collaboration), Phys. Rev. C **47**, 1447 (1993).
[8] G. Royer, J. Phys. G: Nucl. Part. Phys. **26**, 1149 (2000).
[9] N. D. Schubert and M. A. Reyes, At. Data Nucl. Data Tables **93**, 907 (2007)
[10] R. Moustabchir and G. Royer, Nucl. Phys. A **683**, 266 (2001).
[11] P. Mohr, Eur. Phys. J. A **31**, 23 (2007).
[12] L. L. Li, S. G. Zhou, E. G. Zhao, and W. Scheid, Int. J. Mod. Phys. E **19**, 359 (2010).
[13] W. H. Long, J. Meng, and S. G. Zhou, Phys. Rev. C **65**, 047306 (2002).
[14] V. E. Viola Jr. and G. T. Seaborg, Nucl. Chem. Chin. **28**, 741 (1966).
[15] A. Sobiczewski, Z. Patyk, and S. Cwiok, Phys. Lett. B **224**, 1 (1989).
[16] A. Sobiczewski and A. Parkhomenko, Prog. Part. Nucl. Phys. **58**, 292 (2007).

[17] A. Parkhomenko and A. Sobiczewski, Acta Phys. Pol. B **36**, 3095 (2005).
[18] D. Ni, Z. Ren, T. Dong, and C. Xu, Phys. Rev. C **78**, 044310 (2008).
[19] M. Horoi, B. A. Brown, and A. Sandulescu, J. Phys. G: Nucl. Part. Phys. **30**, 945 (2004).
[20] K. P. Santhosh, S. Sabina, and R. K. Biju, Nucl. Phys. A **825**, 159 (2009).
[21] C. Qi, F. R. Xu, R. J. Liotta, and R. Wyss, Phys. Rev. Lett. **103**, 072501 (2009); C. Qi, F. R. Xu, R. J. Liotta, R. Wyss, M. Y. Zhang, C. Asawatangtrakuldee, and D. Hu, Phys. Rev. C **80**, 044326 (2009).
[22] V. Yu. Denisov and A. A. Khudenko, Phys. Rev. C **79**, 054614 (2009); **82**, 059901 (2010).
[23] G. Royer, Nucl. Phys. A **848**, 279 (2010).
[24] D. N. Poenaru and W. Greiner, *Handbook of Nuclear Physics* (Clarendon Press, Oxford, 1996), Chap. 8.
[25] J. M. Dong, W. Zuo, J. Z. Gu, Y. Z. Wang, and B. B. Peng, Phys. Rev. C **81**, 064309 (2010).
[26] T. Dong and Z. Ren, Phys. Rev. C **82**, 034320 (2010).
[27] P. Möller, J. R. Nix, W. D. Myers, and W. J. Swiatecki, At. Data Nucl. Data Tables **59**, 185 (1995); P. Möller, J. R. Nix, and K. L. Kratz, *ibid.* **66**, 131 (1997).
[28] G. Royer and R. Rousseau, Eur. Phys. J. A **42**, 541 (2009); G. Royer and A. Subercaze, Nucl. Phys. A **917**, 1 (2013).
[29] A. E. L. Dieperink and P. Van Isacker, Eur. Phys. J. A **42**, 269 (2009).
[30] M. Liu, N. Wang, Y. G. Deng, and X. Z. Wu, Phys. Rev. C **84**, 014333 (2011).
[31] N. Wang, M. Liu, X. Z. Wu, and J. Meng, Phys. Lett. B **734**, 215 (2014); http://www.imqmd.com/mass/
[32] A. Bhagwat, Phys. Rev. C **90**, 064306 (2014).
[33] M. W. Kirson, Nucl. Phys. A **798**, 29 (2008).
[34] S. Goriely, Nucl. Phys. A **933**, 68 (2014); http://www-astro.ulb.ac.be/bruslib/nucdata
[35] http://www-phynu.cea.fr/science_en_ligne/carte_potentiels_microscopiques/carte_potentiel_nucleaire.htm
[36] J. S. Zheng, N. Y. Wang, Z. Y. Wang, Z. M. Niu, Y. F. Niu, and B. Sun, Phys. Rev. C **90**, 014303 (2014).
[37] Y. Aboussir, J. M. Pearson, and A. K. Dutta, At. Data Nucl. Data Tables **61**, 127 (1995).
[38] M. Liu, N. Wang, and Z. X. Li, Nucl. Phys. A **768**, 80 (2006).
[39] L. S. Geng, H. Toki, and J. Meng, Prog. Theor. Phys. **113**, 785 (2005).
[40] X. Y. Qu, Y. Chen, S. Q. Zhang *et al.*, Sci. China Phys. Mech. Astron. **56**, 2031 (2013).
[41] J. Duflo and A. P. Zuker, Phys. Rev. C **52**, R23 (1995); http://amdc.in2p3.fr/web/dz.html
[42] C. Qi, J. Phys. G: Nucl. Part. Phys. **42**, 045104 (2015).
[43] H. Koura, T. Tachibana, and M. Uno, Prog. Theor. Phys. **113**, 305 (2005).
[44] R. C. Nayak and L. Satpathy, At. Data Nucl. Data Tables **98**, 616 (2012).
[45] M. Bao, Z. He, Y. Lu, Y. M. Zhao, and A. Arima, Phys. Rev. C **88**, 064325 (2013); Y. Y. Cheng, Y. M. Zhao, and A. Arima, *ibid.* **89**, 061304(R) (2014).
[46] Y. Qian and Z. Ren, Eur. Phys. J. A **49**, 5 (2013).
[47] X. Bao, H. Zhang, J. Dong, J. Li, and H. Zhang, Phys. Rev. C **89**, 067301 (2014).
[48] K. P. Santhosh and B. Priyanka, Nucl. Phys. A **929**, 20 (2014).
[49] K. P. Santhosh and B. Priyanka, Phys. Rev. C **89**, 064604 (2014).
[50] D. N. Poenaru, R. A. Gherghescu, and W. Greiner, Phys. Rev. Lett. **107**, 062503 (2011).
[51] D. N. Poenaru, R. A. Gherghescu, and W. Greiner, Phys. Rev. C **85**, 034615 (2012).
[52] V. Yu. Denisov and A. A. Khudenko, Phys. Rev. C **81**, 034613 (2010).
[53] Y. Z. Wang, J. Z. Gu, J. M. Dong, and B. B. Peng, Eur. Phys. J. A **44**, 287 (2010).
[54] Y. Z. Wang, J. Z. Gu, J. M. Dong, and B. B. Peng, Int. J. Mod. Phys. E **19**, 1961 (2010).
[55] Y. Z. Wang, Q. F. Gu, J. M. Dong, and B. B. Peng, Int. J. Mod. Phys. E **20**, 127 (2011).
[56] Y. Z. Wang, Z. Y. Li, G. L. Yu, and Z. Y. Hou, J. Phys. G: Nucl. Part. Phys. **41**, 055102 (2014).
[57] S. Hofmann, Rep. Prog. Phys. **61**, 639 (1998).
[58] S. Hofmann and G. Munzenberg, Rev. Mod. Phys. **72**, 733 (2000).
[59] Yu. Ts. Oganessian, V. K. Utyonkov, Yu. V. Lobanov *et al.*, Phys. Rev. C **62**, 041604 (2000).
[60] Yu. Ts. Oganessian, J. Phys. G: Nucl. Part. Phys. **34**, R165 (2007).
[61] Yu. Ts. Oganessian, Radiochim. Acta **99**, 429 (2011).
[62] Yu. Ts. Oganessian, Nucl. Phys. News **23**, 15 (2013).
[63] J. Khuyagbaatar *et al.*, Phys. Rev. Lett. **112**, 172501 (2014).
[64] K. Morita, K. Morimoto, D. Kaji *et al.*, J. Phys. Soc. Jpn. **73**, 2593 (2004); **81**, 103201 (2012).
[65] Z. Y. Zhang, Z. G. Gan, L. Ma *et al.*, Chin. Phys. Lett. **29**, 012502 (2012).
[66] J. Erler, N. Birge, M. Kortelainen *et al.*, Nature (London) **486**, 509 (2012).
[67] A. Sobiczewski and Yu. A. Litvinov, Phys. Rev. C **89**, 024311 (2014); **90**, 017302 (2014).
[68] N. D. Schubert, M. A. Reyes, and V. A. Tamez, Eur. Phys. J. A **42**, 121 (2009).
[69] D. N. Poenaru, R. A. Gherghescu, and N. Carjan, Europhys. Lett. **77**, 62001 (2007).
[70] J. M. Dong, H. F. Zhang, Y. Z. Wang *et al.*, Nucl. Phys. A **832**, 198 (2010).
[71] Z. Y. Wang, Z. M. Niu, Q. Li, and J. Y. Guo, J. Phys. G: Nucl. Part. Phys. **42**, 055112 (2015).
[72] Y. Qian and Z. Ren, Phys. Rev. C **85**, 027306 (2012).
[73] Y. Ren and Z. Ren, Phys. Rev. C **85**, 044608 (2012).
[74] Y. Z. Wang, J. M. Dong, B. B. Peng, and H. F. Zhang, Phys. Rev. C **81**, 067301 (2010).
[75] Y. Z. Wang, J. Z. Gu, and Z. Y. Hou, Phys. Rev. C **89**, 047301 (2014).
[76] M. Wang, G. Audi, A. H. Wapstra, F. G. Kondev, M. Maccormick, X. Xu, and B. Pfeiffer, Chin. Phys. C **36**, 1603 (2012).
[77] Z. G. Gan, Z. Qin, H. M. Fan *et al.*, Eur. Phys. A **10**, 21 (2001).
[78] Z. G. Gan, J. S. Guo, X. L. Wu *et al.*, Eur. Phys. A **20**, 385 (2004).
[79] Ch. E. Düllmann, W. Brüchle, R. Dressler *et al.*, Nature (London) **418**, 859 (2002).
[80] J. Dvorak, W. Brüchle, M. Chelnokov *et al.*, Phys. Rev. Lett. **100**, 132503 (2008).
[81] P. A. Wilk, K. E. Gregorich, A. Türler *et al.*, Phys. Rev. Lett. **85**, 2697 (2000).
[82] Yu. Ts. Oganessian, V. K. Utyonkoy, Yu. V. Lobanov *et al.*, Phys. Rev. C **69**, 021601(R) (2004).
[83] Yu. Ts. Oganessian, V. K. Utyonkov, Yu. V. Lobanov *et al.*, Phys. Rev. C **70**, 064609 (2004).

[84] Yu. Ts. Oganessian, V. K. Utyonkov, S. N. Dmitriev *et al.*, Phys. Rev. C **72**, 034611 (2005).
[85] Yu. Ts. Oganessian, V. K. Utyonkov, Yu. V. Lobanov *et al.*, Phys. Rev. C **76**, 011601(R) (2007).
[86] Yu. Ts. Oganessian, F. Sh. Abdullin, S. N. Dmitriev *et al.*, Phys. Rev. Lett. **108**, 022502 (2012).
[87] Yu. Ts. Oganessian, V. K. Utyonkov, Yu. V. Lobanov *et al.*, Phys. Rev. C **74**, 044602 (2006).
[88] P. A. Ellison, K. E. Gregorich, J. S. Berryman *et al.*, Phys. Rev. Lett. **105**, 182701 (2010).
[89] Ch. E. Düllmann, M. Schädel, A. Yakushev *et al.*, Phys. Rev. Lett. **104**, 252701 (2010).